Liquid Crystals

Deutsche Ausgabe: DOI: 10.1002/ange.201502440
Internationale Ausgabe: DOI: 10.1002/anie.201502440

A Twist-Bend Nematic (N_{TB}) Phase of Chiral Materials**

Ewa Gorecka, Nataša Vaupotič, Anna Zep, Damian Pociecha, Jun Yoshioka, Jun Yamamoto, and Hideo Takezoe*

Abstract: *New chiral dimers consisting of a rod-like and cholesterol mesogenic units are reported to form a chiral twist-bend nematic phase (N_{TB}*) with heliconical structure. The compressibility of the N_{TB} phase made of bent dimers was found to be as large as in smectic phases, which is consistent with the nanoperiodic structure of the N_{TB} phase. The atomic force microscopy observations in chiral bent dimers revealed a periodicity of about 50 nm, which is significantly larger than the one reported previously for non-chiral compounds (ca. 10 nm).*

There is a growing number of reports on achiral compounds that display a new type of nematic phase, having a chiral structure.[1,2] The existence of such a phase, named the "twist-bend nematic (N_{TB})" is an intriguing and unique example of spontaneous mirror symmetry breaking that occurs in a fluidic state. The question about mechanism that might lead to formation of chiral structures in achiral liquid is of fundamental importance. It is also important to understand how weak chiral interactions manifest themselves in such structures. Transmission electron microscopy (TEM)[1–3] and atomic force microscopy (AFM)[4] measurements showed that the wavelength of spatial helical modulations in the N_{TB} phase is extremely short, just about 3 molecular lengths. Such a short pseudo-layer structure is responsible for characteristic focal conic textures of the N_{TB} phase.[4,5] The short heliconical structure, with the director inclined from the helix axis by an angle lower than 90 deg (oblique helix) is believed to be formed because of a negative bend elastic constant[6] or a large flexoelectric effect.[7,8] Such conditions are realized for the bent molecules, for example dimers with rigid cores connected by sufficiently flexible linkers with an odd number of carbon atoms[9] or hydrogen bonds,[10] and bent-core molecules.[11] Since the heliconical structure of the N_{TB} phase is not related to molecular chirality, the obvious question arises: what effect does the molecular chirality would have on the heliconical structure? So far only one report was published, in which the authors showed that for chiral twin molecules the strong competition between the effects induced by chirality and molecular bend might lead to a sequence of modulated nematic phases with distinct phase transitions in a narrow temperature range between the regular cholesteric phase (N*) and new nematic phase, preliminarily identified as a "splay-bend" nematic structure,[12] in agreement with theoretical predictions.[13] Here we extend our studies to several chiral dimeric materials showing the N-N phase transition; by miscibility studies the lower-temperature nematic phase was identified as the N_{TB} phase and the upper temperature phase as a cholesteric one.

Asymmetric bi-mesogens are studied, in which rod-like units, azo (**Azo** series) or imine (**SB** series), are connected with a cholesteric unit by an alkyl spacer with an odd number of carbon atoms (Figure 1, for synthesis details see the Supporting Information). Such molecular geometry promotes bent conformers, in which two mesogenic units make an average angle of 120 deg; it also ensures large flexibility because of a low energy barrier for rotations around chemical bonds within the spacer. Two basic molecular modifications were applied for both series of compounds; the length (n) of a terminal alkyl or alkoxy chain at the rod-like azo/imine unit and the length of the flexible spacer (m) were changed. For a fixed terminal chain ($n=1$), compounds show the N*-N_{TB}* phase transition, except for the azo compound with the longest $m=15$ tail, for which the N*-SmA phase transition was found (related DSC scans are presented in the Supporting Information). Apparently changing the length of the inner spacer does not influence much the phase sequence. On the contrary, extending the terminal alkyl chain (for a chosen spacer length, $m=5$) exerts much more profound influence on the phase sequence; the N_{TB}* phase was stable only for short homologues, $n=1$–3 for imine and only for $n=1$ for azo derivatives. The homologues with alkyl tails longer than $n=4$ for imine and $n=2$ for azo derivatives show complex sequences of modulated smectic phases. The phase sequence for studied compounds is presented in Figure 1.

In the lower-temperature nematic phase the viscosity was comparable to the viscosity of the smectic phase, but the X-

[*] Prof. E. Gorecka, A. Zep, Dr. D. Pociecha, Prof. H. Takezoe
Department of Chemistry, Warsaw University
ul. Zwirki i Wigury 101, 02-089 Warsaw (Poland)
E-mail: gorecka@chem.uw.edu.pl
Prof. N. Vaupotič
Faculty of Natural Sciences and Mathematics
University of Maribor, Koroška 160, Maribor (Slovenia)
and
Jozef Stefan Institute
Jamova 39, 1000 Ljubljana (Slovenia)
Dr. J. Yoshioka
Department of Physics and Applied Physics
Waseda University
3-4-1 Okubo, Shinjuku-ku, Tokyo169-8555 (Japan)
Prof. J. Yamamoto
Department of Physics, Kyoto University
Kitashirakawaoiwake-cho, Sakyo-ku, Kyoto
606-8502 (Japan)
Prof. H. Takezoe
Toyota Physical and Chemical Research Institute
41-1, Yokomichi, Nagakute, Aichi 480-1192 (Japan)

[**] This work was financed by Foundation for Polish Science under program MASTER 3/2013 and the research program P1-0055 financed by the Slovenian Research Agency.

Supporting information for this article is available on the WWW under http://dx.doi.org/10.1002/anie.201502440.

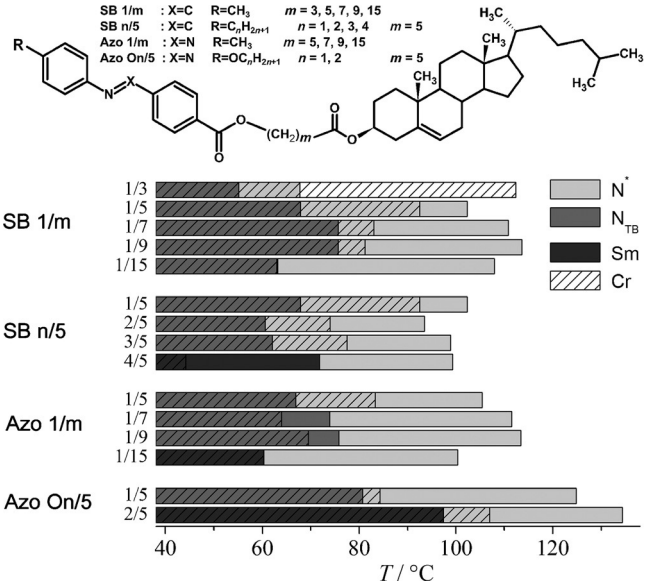

Figure 1. Molecular structure and phase diagrams for the studied materials; the length (*n*) of a terminal alkyl or alkoxy chain at the rod-like azo/imine unit and the length of the flexible spacer (*m*) were varied. The hatched areas give the temperature stability of crystal phase in heating run.

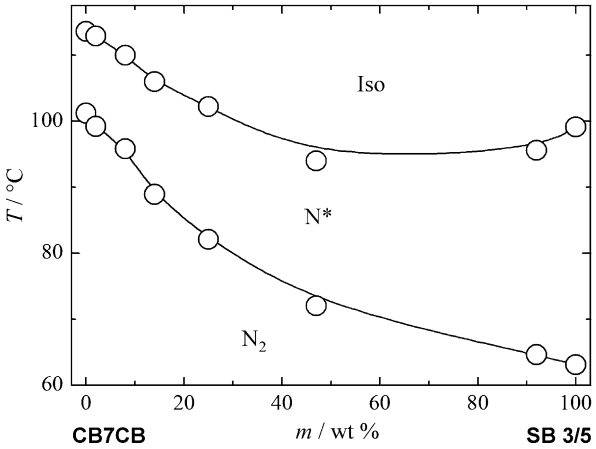

Figure 2. Phase diagram for binary mixtures of model N_{TB} material **CB7CB** and chiral dimer **SB 3/5** showing miscibility in both upper and lower temperature nematic phases.

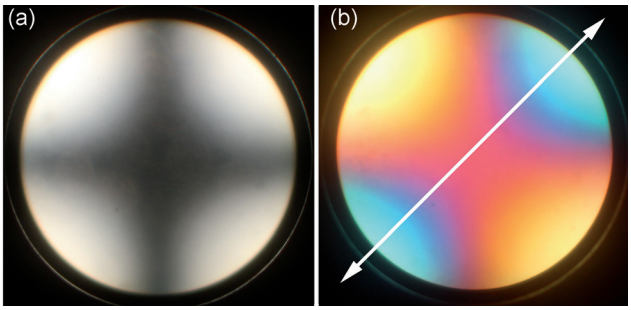

Figure 3. Conoscopic picture in the N_{TB}* phase of **SB 3/5** at room temperature a) without and b) with λ-plate inserted into optical path. The arrow indicates the direction of the slow axis of a λ plate; the position of the colors with respect to the direction of the λ-plate indicates that the material is optically positive.

ray investigations excluded the layered structure (see the Supporting Information). In both nematic phases, weak diffused signals corresponding nearly to a half and full molecular length were detected and the positional correlation length determined from the width of the signal was approximately one molecular length in the N* phase. The signal that is related to a full molecular length became slightly narrower in the lower-temperature nematic phase, but the correlation length (ca. 1.5 molecular length) remained typical for the liquid phase.

To identify the lower-temperature nematic phase in the chiral bent dimers, a miscibility test was conducted using model N_{TB} mesogen **CB7CB**[1,5] and **SB 3/5** compound. Despite of much different textures (see the Supporting Information)—for chiral dimers typically non-birefringent texture while for a non-chiral **CB7CB** dimer usually arrays of focal conic domains were detected—the miscibility studies (Figure 2) showed that the lower temperature nematic phase of the chiral bent dimer and the N_{TB} phase are miscible. The N*-N_{TB}* transition temperature changes monotonically with the mixing ratio as well as the pitch of cholesteric phase.

Microscope observations for the studied chiral dimers in glass cells with planar anchoring revealed that in both nematic phases the optical axis was aligned perpendicular to the glass substrates, and the transition to the N_{TB}* was marked by a sudden disappearance of optical activity. The conoscopic image (Figure 3) clearly shows that the N_{TB}* phase is uniaxial with the positive optical anisotropy, contrary to the N* phase having the negative optical anisotropy. Because in the N_{TB}* phase the refractive index is larger along the helical axis, the conical angle of the helical structure must be less than magic angle 54 degrees. This value of conical angle is consistent with the previous measurements (ca. 30 degree) in the non-chiral N_{TB} phase reported by Meyer et al.[14]

To obtain more information on the periodic structure of the N_{TB} and N_{TB}* phases, compression modulus studies were performed for **CB7CB** and **SB 3/5** compounds. As shown in Figure 4 (inset), the upper-temperature nematic phase has

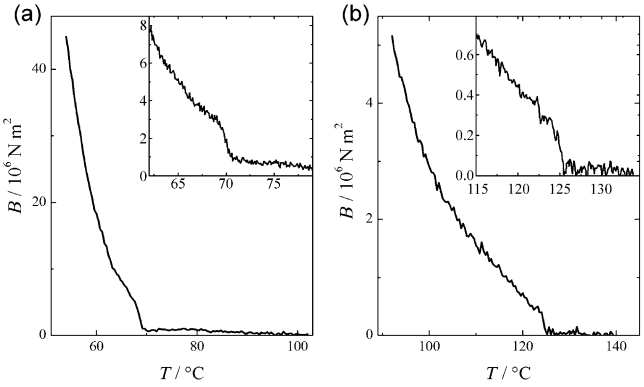

Figure 4. Compression modulus constant (*B*) versus temperature (*T*) in a) **SB 3/5** and b) **CB7CB** material.

very small compression modulus, that is, B is about 5×10^5 Pa for **SB 3/5** and almost zero for **CB7CB**, as expected for the cholesteric phase with a helix of a pitch within the range of optical wavelengths and the nematic phase, which is not compressible, respectively. The value of B rises stepwise at the N(*)-N_{TB}(*) phase transition to 2×10^6 Pa for **SB 3/5** and 2×10^5 Pa for **CB7CB**, and further sharply increases with lowering temperature (Figure 4) reaching the values 4×10^7 Pa in the N_{TB}* phase of **SB 3/5** and 4×10^6 Pa in the N_{TB} phase of **CB7CB**. In both, **CB7CB** and **SB 3/5**, the values of B that are typical for smectic phases[15,16] were measured. The lower value of B found for **CB7CB** compared with **SB 3/5** might be due to the problems with sample alignment—nearly ideal homeotropic orientation, which is required for high quality modulus measurements, was easily obtained for the **SB 3/5**, whereas for **CB7CB** the homeotropic orientation was not perfect. The value of B in the range of 10^7 Pa is typical for smectic phases, while the compressibility of non-modulated nematic phase is practically zero.

Because there is no long-range positionally ordered structure in the N_{TB}(*) phase, the value of B of the order of 10^6 Pa must reflect an existence of a periodic orientational structure with a nanometer length scale for both chiral and nonchiral materials. The nearly linear and monotonic increase of B within the N_{TB}(*) phase temperature range might be attributed for example to quantitative changes of heliconical structure.

The high viscosity of the **SB 3/5** imine material and stability of the N_{TB}* phase at room temperature even for days, despite being monotropic, enabled detailed AFM studies. The AFM images obtained in the chiral N_{TB}* phase depended on the sample preparation process. If the sample was prepared between glass plates with planar anchoring, opened and immediately examined by AFM, a smooth surface was detected. However, if the sample with one free surface was heated above the N_{TB}*-N* transition and subsequently cooled down and kept at room temperature for few hours, tiny and birefringent mosaic textures developed. The AFM images of such samples revealed a fingerprint pattern (Figure 5a), similar to those observed in the cholesteric phase (see the Supporting Information). As discussed in a number of papers related to the long-pitch cholesteric materials,[17,18] such patterns develop when the free surface favors parallel orientation of the helical axis with respect to the surface. The closest distance between the fingerprint lines in the N_{TB}* phase was 50–60 nm, which gives the longest limit of the pitch. It should be stressed that this value is much longer than the periodicity in the N_{TB} phase of **CB7CB** material, which is about 8 nm (Figure 5b). The AFM studies were also conducted for the mixtures of **SB 3/5** and **CB7CB.** For a low concentration of **SB 3/5** (up to a few %) in the planar cell the focal conic textures were clearly detected, confirming the short periodicity of the structure. However, the equidistant lines, that were clearly visible by AFM in the pure **CB7CB** material (Figure 5b), could not be detected in the images of the mixtures. Instead, focal conics are covered by irregular defect lines (Figure 5c) similarly as observed for focal conics in a chiral smectic phase with a long pitch, when the pitch is partially unwound due to the interactions with the surface.[19]

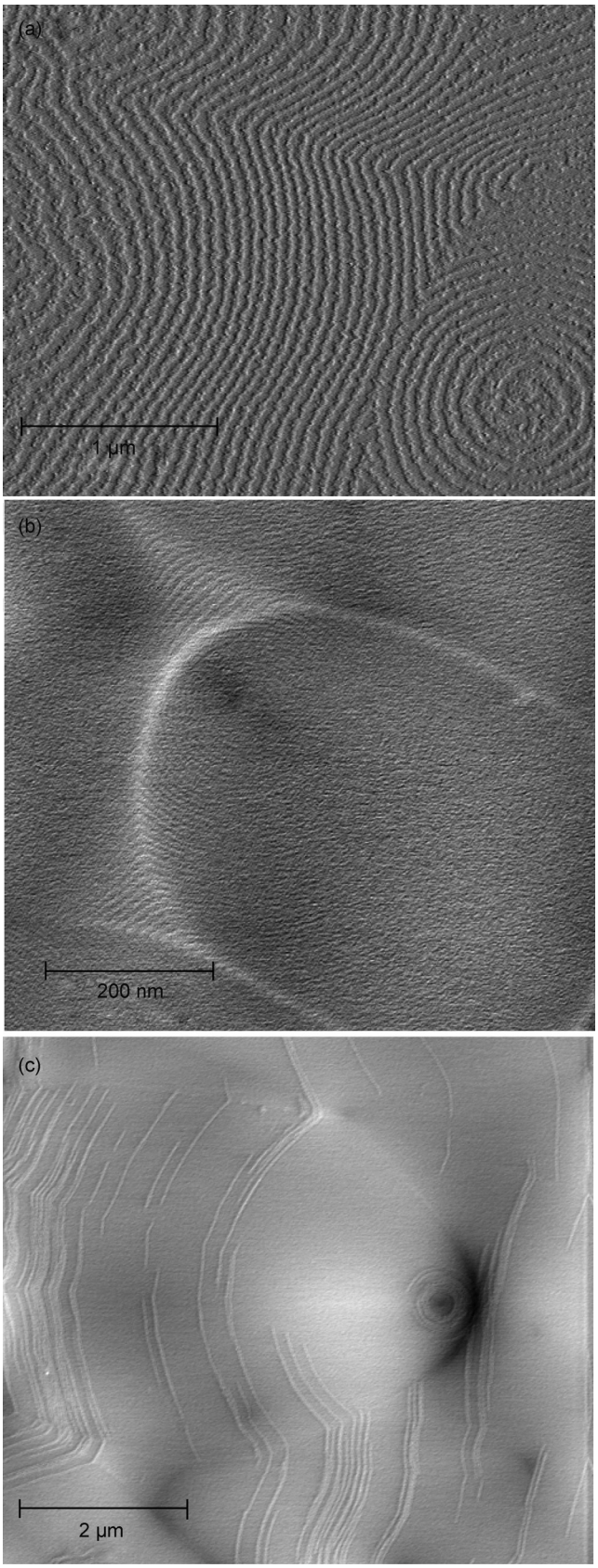

Figure 5. AFM pictures in a) the N_{TB}* phase of material **SB 3/5**, b) in N_{TB} phase of material **CB7CB** and c) for a mixture of **CB7CB** with 5% of **SB 3/5.**

The theoretical description of the observed structures and their properties was suggested by Meyer et al.[7] and revived by Selinger and co-workers.[8] The driving mechanism responsible for formation of N_{TB} is the flexoelectric effect that connects the director field gradient with the generation of the electric polarization. The free energy density for non-chiral system can be expressed as shown in Equation (1),

$$f = \frac{1}{2}K_1\left(\nabla\cdot\vec{n}\right)^2+\frac{1}{2}K_2\left(\vec{n}\cdot\left(\nabla\times\vec{n}\right)\right)^2+\frac{1}{2}K_3\left(\vec{n}\times\left(\nabla\times\vec{n}\right)\right)^2+ \lambda p_0\vec{p}\cdot\left(\vec{n}\times\left(\nabla\times\vec{n}\right)\right)+\frac{1}{2}\mu(T)p_0^2+\frac{1}{2}\kappa p_0^2\left(\left(\nabla\cdot\vec{p}\right)^2+\left(\nabla\times\vec{p}\right)^2\right) \quad (1)$$

where the director $\vec{n}$ points along the local orientation of the long molecular (dimer) axis and $\vec{p}$ is a director along the local flexoelectric polarization. The magnitude of the local polarization is p_0; K_1, K_2 and K_3 are the splay, twist and bend elastic constants, respectively, for the deformation in the director $\vec{n}$. The structure is locally biaxial, which is taken into account by additional elastic constant κp_0^2, which gives the cost of the splay, bend and twist deformation of the polar director $\vec{p}$; in such a way the enormous number of elastic constants that are required to describe properly biaxial nematic structure is reduced. It is also assumed that the elastic constant describing the cost of spatial variation of $\vec{p}$ depends on the magnitude of polarization. The λ term describes the flexoelectric and the $\mu(T)$ term—the dielectric contribution to the free energy. The dielectric susceptibility is temperature dependent; it reduces with decreasing temperature. When temperature is low enough, the flexoelectric term stabilizes the twist-bend structure.[8,13] To estimate the compressibility of the short pitch oblique helix in the twist-bend nematic phase, the following ansatz is used [Eq. (2)],

$$\vec{n} = (\cos\theta, \sin\theta\sin qx, \sin\theta\cos qx)$$
$$\vec{p} = (0, -\cos qx, \sin qx) \quad (2)$$

where θ is the conical angle and q is the short pitch modulation wave vector, the helical axis is along the x-direction. We assume that $\vec{p}$ is in the direction of the dimer kink, because the molecular dipole is expected to be largest in this direction.[13] For small θ the twist-bend structure is stabilized if $\mu(T) < \frac{\lambda^2}{K_3}$, so we express $\mu(T)$ as given by Equation (3),

$$\mu(T) = c(T)\frac{\lambda^2}{K_3} \quad (3)$$

where $c(T)$ is a temperature dependent parameter, which equals 1 at the phase transition from the nematic to the twist-bend nematic phase and 0 at the transition to a virtual, truly polar nematic. The following expressions are obtained for the equilibrium values p_0, θ_0 and q_0, assuming that $\theta \ll 1$ [Eq. (4)].

$$\theta_0 = \sqrt{\frac{1-c}{-2+\frac{3K_2}{K_3}-2c}}$$
$$p_0 = \sqrt{\frac{K_3}{\kappa}}\sqrt{1-c\theta} \quad (4)$$
$$q_0 = \sqrt{\frac{(1-c)\lambda^2}{\kappa K_3}}$$

Assuming small variation of θ from its equilibrium value, $\theta = \theta_0 + \delta\theta$, the compressibility modulus B, which is the term in the free energy in front of $(\delta\theta)^2$ can be given by Equation (5).

$$B = 4K_2\theta_0^2q_0^2 \quad (5)$$

As c reduces with decreasing temperature, q_0, θ, and B increase. We point out that although the model is very crude it gives the proper temperature dependence of B in the N_{TB} phase (where B steeply increases as about $1/T$) already by assuming a linear dependence of c on T.

Assuming $K_2 = K_3$, taking $B = 10^6$ Pa, $q_0 = 2\pi/d_0$ where $d_0 = 8$ nm and $\theta = 30$ deg we find $c = 0.5$ and the correct order of magnitude for $K_2 \approx 2\times10^{-12}$ N and $\frac{\lambda^2}{\kappa} \approx 10^5$ Pa. Since for the other non-chiral materials the pitch in the N_{TB} is of the same order of magnitude[2] as for **CB7CB** it is likely that the ratio between the λ^2—flexoelectric and κ—splay of local polarization constants of the order of 10^5–10^6 is general and governs compressibility of the N_{TB} phase.

By adding a chiral term to the free energy density expression only a slight modification of the pitch (by maximum 30%) is predicted while the experiment gives a pitch, which is by an order of magnitude longer. Thus to give a better description of the chiral system, the biaxial model reported in Ref. [13] was applied. The ratio between the pitch in the N* and N_{TB}* phase is $\frac{k_1+k_2}{k_1+k_3}$ (see Eqs. (4) and (13) in Ref. [13]), where k_3 is a chiral parameter for the twist of director $\vec{n}$, k_1 for the twist of $\vec{l}$ (the director perpendicular to $\vec{n}$ in the direction of the dimer kink), and k_2 for the twist of the director perpendicular to $\vec{n}$ and $\vec{l}$. Experiment suggests that k_1 and k_3 are of the opposite sign,[12] and thus the pitch in the N_{TB}* phase might be very different from the one in the N* phase. By using the biaxial model[13] and applying the same procedure as for the achiral case, we find the expression for the compressibility of the chiral twist-bend nematic phase [Eq. (6)].

$$B = 8Kq_0^2\frac{1-c}{c}\frac{k_2-k_3}{k_1+k_2} \quad (6)$$

B is temperature dependent and increases as about $1/T$ when temperature decreases, assuming a linear dependence of c on T. Taking $K \approx 1$ pN and $d_0 = 50$ nm, we find $8Kq_0^2 \approx 10^5$ Pa. It is highly unlikely that the ratio among the chiral elastic parameters would bring another 2 orders of magnitude, which would then lead us to the experimentally measured order of magnitude of B. But we point out that the one-elastic-constant approximation is an oversimplification. The ratio among elastic constants can easily bring another order of magnitude;

however the model becomes too complex to be considered herein.

Summarizing, the studies show that the achiral and chiral forms of N_{TB} are thermodynamically identical phases, like the N and N* phases. Contrary to N* phase, the structure of N_{TB}* is optically positive, thus the conical angle of the heliconical structure is less than the magical angle. The high compression moduli, which are in the same range as for smectic phases, indicate a structure with a periodicity in a nanometer range. For chiral materials the periodicity observed by AFM is about 50 nm and corresponds to 10–15 molecular lengths, which is considerably longer than that in achiral compound **CB7CB** (three molecular lengths).

Keywords: atomic force microscopy · chirality · liquid crystals · spontaneous symmetry breaking · X-ray diffraction

How to cite: *Angew. Chem. Int. Ed.* **2015**, *54*, 10155–10159
Angew. Chem. **2015**, *127*, 10293–10297

[1] D. Chen, J. H. Porada, J. B. Hooperc, A. Klittnick, Y. Shen, M. R. Tuchband, E. Korblova, D. Bedrov, D. M. Walba, M. A. Glaser, J. E. Maclennan, N. A. Clark, *Proc. Natl. Acad. Sci. USA* **2013**, *110*, 15931.
[2] V. Borshch, Y.-K. Kim, J. Xiang, M. Gao, A. Jákli, V. P. Panov, J. K. Vij, C. T. Imrie, M. G. Tamba, G. H. Mehl, O. D. Lavrentovich, *Nat. Commun.* **2013**, *4*, 2635.
[3] Y. Wang, G. Singh, D. M. Agra-Kooijman, M. Gao, H. K. Bisoyi, Ch. Xue, M. R. Fisch, S. Kumar, Q. Li, *Cryst. Eng. Comm.* **2015**, DOI: 10.1039/c4ce02502d.
[4] E. Gorecka, M. Salamonczyk, A. Zep, D. Pociecha, C. Welch, A. Ziauddin, G. H. Mehl, *Liquid Cryst.* **2015**, *42*, 1–7.
[5] V. P. Panov, M. Nagaraj, J. K. Vij, Y. P. Panarin, A. Kohlmeier, M. G. Tamba, R. A. Lewis, G. H. Mehl, *Phys. Rev. Lett.* **2010**, *105*, 167801.
[6] I. Dozov, *Europhys. Lett.* **2001**, *56*, 247.
[7] R. B. Meyer, in *Molecular Fluids* (Eds.: R. Balian, G. Weill), Gordon and Breach, New York, **1976**, vol. XXV-1973 of Les Houches Summer School in Theoretical Physics, pp. 273–373.
[8] S. M. Shamid, S. Dhakal, J. V. Selinger, *Phys. Rev. E* **2013**, *87*, 052503.
[9] R. J. Mandle, E. J. Davis, S. A. Lobato, C. C. A. Vol, S. J. Cowling, J. W. Goodby, *Phys. Chem. Chem. Phys.* **2014**, *16*, 6907.
[10] S. M. Jansze, A. Martinez-Felipe, J. M. D. Storey, A. T. M. Marcelis, C. T. Imrie, *Angew. Chem. Int. Ed.* **2015**, *54*, 643; *Angew. Chem.* **2015**, *127*, 653.
[11] D. Chen, M. Nakata, R. Shao, M. R. Tuchband, M. Shuai, U. Baumeister, W. Weissflog, D. M. Walba, M. A. Glaser, J. E. Maclennan, N. A. Clark, *Phys. Rev. E* **2014**, *89*, 022506.
[12] A. Zep, S. Aya, K. Aihara, K. Ema, D. Pociecha, K. Madrak, P. Bernatowicz, H. Takezoe, E. Gorecka, *J. Mater. Chem. C* **2013**, *1*, 46.
[13] N. Vaupotič, M. Čepič, M. Osipov, E. Gorecka, *Phys. Rev. E* **2014**, *89*, 030501.
[14] C. Meyer, G. R. Luckhurst, I. Dozov, *J. Mater. Chem. C* **2015**, *3*, 318.
[15] J. Yamamoto, K. Okano, *Jpn. J. Appl. Phys.* **1991**, *30*, 754.
[16] S. Shibahara, Y. Takanishi, J. Yamamoto, T. Ogasawara, K. Ishikawa, H. Yokoyama, H. Takezoe, *Phys. Rev. E* **2001**, *63*, 062701.
[17] A. Bobrovsky, O. Sinitsyna, S. Abramchuk, I. Yaminsky, V. Shibaev, *Phys. Rev. E* **2013**, *87*, 012503.
[18] G. Agez, R. Bitar, M. Mitov, *Soft Matter* **2011**, *7*, 2841.
[19] M. Glogarová, J. Pavel, *J. Phys. (Paris)* **1984**, *45*, 143.

Received: March 17, 2015
Revised: May 22, 2015
Published online: July 14, 2015

